Li^+ Ion Affinities of Global-Warming Perfluorocarbons

Sundaram Arulmozhiraja and Toshihiro Fujii*

Environmental Chemistry Division, National Institute for Environmental Studies, 16-2 Onogawa, Tsukuba, Ibaraki 305-0053, Japan

Received: May 22, 2000; In Final Form: August 14, 2000

Density functional theory studies were performed for the first time to obtain the Li^+ ion affinities of various perfluorocarbons (PFCs) that cause global-warming. Becke's three-parameter hybrid density functional, B3LYP combined with 6-31G(d), 6-311+G(2d), and 6-311+G(3df) basis sets were utilized for this purpose. We present optimized geometries of PFC−Li^+ ion complexes at B3LYP/6-311+G(2d) level. The frequencies obtained at the same level were used to verify all the optimized geometries are minima. The following PFCs—CF_4, CHF_3, CH_2F_2, CH_3F, C_2F_6, C_4F_8, with SF_6—were considered in the present study. The calculated Li^+ affinities for CF_4, CHF_3, CH_2F_2, CH_3F, C_2F_6, C_4F_8, and SF_6 are 12.31, 19.64, 26.84, 30.10, 17.20, 21.09, and 16.92 kcal/mol, respectively at B3LYP/6-311+G(3df) after zero-point energy and thermal energy corrections. The large Li^+ affinities indicate the validity of our proposed Li^+ ion attachment mass spectrometry to quantify the emission of these greenhouse gases from semiconductor industries. Complex geometries were obtained and the ion−molecular bonding nature was discussed on the basis of atomic charge, electron density ρ, and its Laplacian.

Introduction

Global-warming is one of the major threats humankind is presently facing. In addition to naturally available greenhouse gases, such as carbon dioxide, methane and nitrous oxide, man-made greenhouse gases contribute significantly to the global-warming process.[1,2] Hydrofluorocarbons (HFCs) and perfluorocarbons (PFCs) are potent greenhouse gases produced by industries. These gases, plus sulfur hexafluoride (the most potent greenhouse gas),[2] play a significant role in the global-warming process. Furthermore, these compounds have extremely long atmospheric lifetimes, resulting in their essentially irreversible accumulation within the atmosphere.

Many PFCs have important and wide-ranging uses in industry, particularly in plasma industries and semiconductor technology.[3] Unfortunately, most of them are greenhouse gases. The commonly used PFCs in industries are CF_4, CHF_3, and C_2F_6. The global-warming potential (GWP) of these greenhouse gases is very high, and they have long lifetimes. The atmospheric half-lives of CF_4, CHF_3, and C_2F_6 are 50000, 250, and 10000 years, respectively, and their GWPs over a one-hundred year period are 6300, 12100, and 12200, respectively, with reference to the absolute global-warming potential for CO_2.[2,4−6]

Hence, controlling the production of PFCs in industry is essential to reduce global-warming. However, complete control is difficult, and the Intergovernmental Panel on Climate Change (IPCC) has proposed some regulations on production levels of these gases.[2] Thus, quantitative analysis of the emission of PFCs from industry is timely. Electron impact mass spectrometry is often employed for such studies, however, most PFCs dissociate or predissociate with high probability; hence, the parent molecular ions must be unstable and were not observed experimentally.[7−14] Electron impact ionization produces many neutral radicals and ions. This may create difficulty in quantitative analysis and the situation is further complicated as most of PFCs break into similar fragments.[12−14] Therefore Harnisch et al.[15] employed mass spectrometry combined with a GC and/or a cryotrap technique for the measurements of CF_4, SF_6, and C_2F_6 in the atmosphere.

Li^+ ion attachment mass spectrometry, developed by one of the present authors, can be a direct method through which one can analyze the sample without any refinement such as separation of the sample from the abundant atmospheric species.[16−29] It permits sampling at atmospheric pressure followed by soft ionization mass spectrometry. Sample gases are introduced through a small aperture at atmospheric pressure into an ionization chamber containing a lithium ion emitter. In this reaction chamber, Li^+ ion attachment to the molecule takes place. The ionized adduct is detected by a quadrupole mass spectrometer. With this instrument incorporating soft ionization, it is possible to detect chemical species on a real-time basis.

Preliminary experiments demonstrate the feasibility of measuring PFCs in exhaust from the semiconductor industry by generating Li^+ ion adducts. No serious interference from more abundant species in air has been observed because of the generation of ions which do not get fragmented. High sensitivity warrants real-time monitoring in the exhaust process. Additional benefits include low background effects and sensitive ionization without any substantial fragmentation in Li^+ ion attachment spectrometry. The applicability of this method depends on the Li^+ ion affinity of PFCs. Although fluorine-containing compounds have higher ion affinities, some of these greenhouse gases have very small polarizability and do not have a permanent dipole moment. To date, only a few studies have been undertaken to obtain the Li^+ ion affinities of PFCs.[30−33] Therefore, a theoretical study on the Li^+ ion affinities of these PFC compounds is highly necessary.

Nowadays, density functional theory (DFT)[34] plays a prominent role in studying the chemistry of molecules. A number of studies have shown that various ion affinities obtained using

---

* Author to whom correspondence should be addressed. Fax: +81-298-2574. E-mail: t-fujii@nies.go.jp.

10.1021/jp0018753 CCC: $19.00

hybrid DFT methods are highly comparable in quality with the experimental values.[35−37] We have used the popular B3LYP hybrid functional in the DFT to calculate the Li^+ ion affinities of various PFCs, including the following PFCs—CF_4, CHF_3, CH_2F_2, CH_3F, C_2F_6, and C_4F_8, along with SF_6 in the present study.

The chemical bonding in various PFCs and the PFC−Li^+ bonding nature were analyzed by studying the electron density (ρ) and its Laplacian ($\nabla^2\rho$). As has been shown by the Bader group,[38−41] $\nabla^2\rho$ identifies regions of space wherein the electronic charge of a system is locally concentrated, $\nabla^2\rho < 0$ or depleted, $\nabla^2\rho > 0$. According to the theory, negative values of $\nabla^2\rho$ at the bond critical point (bcp, where $\nabla\rho = 0$) are associated with shared interactions, typically covalent bonds, while positive $\nabla^2\rho$ values are associated with closed shell interactions, corresponding to ionic bonds, hydrogen bonds, and van der Waals interactions. The concentration of the electronic charge at the bcp is relatively low for closed shell systems and large for shared interactions. Therefore, by analyzing these parameters, ρ and $\nabla^2\rho$ at bond critical points, we can identify the nature of ion−molecular bonding as well as bond activation effects in the ligands upon Li^+ ion attachment.

We have carried out a theoretical study of the Li^+ ion complexes of perfluorocarbons and sulfur hexafluoride in an attempt to understand the applicability of Li^+ ion attachment mass spectrometry to estimate emissions from industry of these global-warming gases. The first priority of the present study was to determine accurate Li^+ ion affinities of these greenhouse gases, i.e., CF_4, CHF_3, C_2F_6, C_4F_8, and SF_6. To ensure the accuracy of the calculated affinities, we have obtained the Li^+ ion affinities of two other perfluorocarbons, CH_2F_2 and CH_3F, for which experimental values are available in the literature.[30,31] The study on these two PFCs also provides a platform to analyze the Li^+ ion affinities due to multiple fluorine substitution on methane. The complex geometries and atomic charges have been presented in this paper. Bader's Atoms-in-Molecules (AIM) theory has been used to characterize the bonding nature.[38−41]

Computational Methodology. All calculations were performed using Gaussian 98 programs.[42] The Becke's three-parameter hybrid density functional, B3LYP, which includes a mixture of Hartree−Fock exchange and DFT exchange correlation has been used. The Becke's three-parameter functional[43] has the form $AE_x^{\text{slater}} + (1 - A)E_x^{\text{HF}} + BE_x^{\text{Becke88}} + E_c^{\text{VWN}} + C\,\Delta E_c^{\text{non-local}}$, where the nonlocal correlation is provided by the Lee−Yang−Parr expression.[44] The constants *A*, *B*, and *C* are those determined by Becke by fitting the results in the G1 molecular set.[43,45]

The ligands, as well as complexes, were optimized first at the B3LYP functional using the 6-31G(d) basis set followed by the frequency calculation, and it was found that none of the ligands and complex structures have any imaginary frequencies and thus all were identified as minima. Second, the 6-311+G(2d) basis set was used to optimize the ligands as well as complex structures. The binding energies (ΔE) were obtained from the difference between the total energy of the complex [E(PFC−Li^+)] and the sum of the total energies of the corresponding Li^+ ion [$E(Li^+)$] and perfluorocarbon [E(PFC)] using the optimized energies: $\Delta E = [E(\text{PFC}-\text{Li}^+)] - \{[E(\text{PFC})] + [E(\text{Li}^+)]\}$. These optimized geometries were characterized by harmonic vibrational frequency calculations at the same B3LYP/6-311+G(2d) level, and these showed all structures were minima on the potential energy surface. These frequency calculations also yielded the zero-point energies (ZPE), which were left unscaled; thermal corrections (at 298.15 K) were needed for the calculation of enthalpies. Binding enthalpies (Li^+ affinities of ligands) were then calculated using the following relation: $\Delta H = \Delta E + \Delta E_{\text{ZPE}} + \Delta E_{\text{thermal}} + \Delta(PV)$, where $\Delta(PV) = nRT = -0.593$ kcal/mol at 298.15 K. Third, Li^+ affinities were calculated using the energies of the optimized structures at B3LYP/6-311+G(3df) level and corrected by ZPE and thermal corrections, which were obtained at B3LYP/6-311+G(2d) level. Atomic charges were derived using the natural population analysis (NPA) scheme.[46,47] Chemical bonding analysis was performed using the AIM keyword option in the Gaussian program.

TABLE 1: Li^+ Ion Affinities (ΔH in kcal/mol) of Different Perfluorocarbans at B3LYP Functional Using Various Basis Sets

	ΔH			
molecule	6-31G(d)	6-311+G(2d)	6-311+G(3df)	expt
CF_4	−20.42	−12.07	−12.31	
CHF_3	−28.80	−19.35	−19.64	
CH_2F_2	−36.47	−26.61	−26.84	−26.5[30,31]
CH_3F	−36.70	−29.95	−30.10	−31.0[30,31]
C_2F_6	−27.33	−16.90	−17.20	
C_4F_8	−34.85	−20.56	−21.09	
SF_6	−24.74	−16.63	−16.92	

Results and Discussions

It is well-known that the fluorine atom is critical with respect to basis set saturation, as well as neglect of electron correlation. Since all the selected molecules in the present study contain fluorine atoms we confirmed our results by calculating the Li^+ ion affinities of CH_3F and CH_2F_2 molecules for which experimental values are available in the literature. There are a few theoretical studies on the CH_3F molecule. Kollman and Rotherberg[32] predicted an affinity value of 39.31 kcal/mol, while the Pople group[33] reported that the result, at the MP2/6-31G* level, was 34.3 kcal/mol. The latter was overestimated by 3.3 kcal/mol. We have used three different basis sets with the B3LYP functional to calculate the Li^+ ion affinities of these PFCs and the results are tabulated in Table 1. The affinity values calculated for CH_3F and CH_2F_2 molecules using both the 6-311+G(2d) and 6-311+G(3df) basis sets with the B3LYP functional coincide well with the experimental values. A maximum difference of 1.05 kcal/mol was seen for CH_3F at the B3LYP/6-311+G(2d) level. Therefore, we are confident that the results obtained for the other PFCs are likely to be highly accurate.

(a) CF_4, CHF_3, CH_2F_2, CH_3F. Much attention has been focused in the past on multiple-substituted methane by electronegative fluorine atoms.[48,49] These fluorine substituents provide lone pairs leading to nonadditive stabilization due to favorable (anomeric) interactions of the adjacent substituents.[50] The generally accepted explanation for the stabilizing effect is negative hyperconjugation.[51,52] Due to this behavior, CF_4 is stabilized by 58 kcal/mol with respect to CH_3F.[53] Stabilization and bond shortening with increasing fluorine substitution at carbon may be attributed to coulombic interactions between negatively charged fluorines and the increasingly positively charged carbon. The present study also shows shortening of C−F bond lengths going from CH_3F (1.392 Å) to CF_4 (1.327 Å) accompanied by an increase in the positive charge on the central carbon atom. This shortening should be reflected in the stability of these molecules, which should increase with increase in fluorine substitution: $CF_4 > CHF_3 > CH_2F_2 > CH_3F$. One can easily understand this behavior by making an analysis of the C−F bonding. Electron density and its Laplacian are more useful than atomic charges. The calculated atomic charges,

TABLE 2: Atomic Charges *q* (in e), Charge Densities *ρ* (in e/au^3), and Laplacian Charge Densities $\nabla^2\rho$ (in e/au^5) Evaluated at the Corresponding Bond Critical Points

Molecule	q	bcp	ρ	$\nabla^2\rho$	Complex	q	bcp	ρ	$\nabla^2\rho$
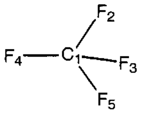	q_{C1} = 1.358 q_{F2} = -0.339	C-F	0.304	-0.660	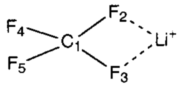	q_{C1} = 1.362 q_{F2} = -0.398 q_{F4} = -0.276 q_{Li^+} = 0.982	C1-F2 C1-F4 F2-Li^+	0.270 0.335 0.176	-0.628 -0.642 0.123
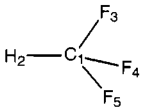	q_{C1} = 0.952 q_{H2} = 0.119 q_{F3} = -0.357	C-H C-F	0.298 0.284	-0.107 -0.490	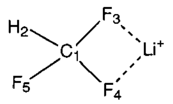	q_{C1} = 0.943 q_{H2} = 0.182 q_{F3} = -0.408 q_{F5} = -0.285 q_{Li^+} = 0.978	C1-H2 C1-F3 C1-F5 F3-Li^+	0.299 0.254 0.318 0.196	-0.112 -0.473 -0.451 0.137
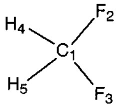	q_{C1} = 0.500 q_{F2} = -0.377 q_{H4} = 0.127	C-F C-H	0.260 0.291	-0.315 -0.101	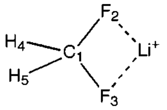	q_{C1} = 0.484 q_{F2} = -0.415 q_{H4} = 0.185 q_{Li^+} = 0.977	C1-F2 C1-H4 F2-Li^+	0.237 0.296 0.216	-0.261 -0.108 0.154
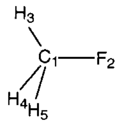	q_{C1} = -0.062 q_{F2} = -0.398 q_{H3} = 0.154	C-F C-H	0.235 0.281	-0.178 -0.939	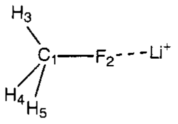	q_{C1} = -0.046 q_{F2} = -0.524 q_{H3} = 0.193 q_{Li^+} = 0.990	C1-F2 C1-H3 F2-Li^+	0.177 0.288 0.373	0.439 -0.100 0.341
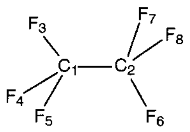	q_{C1} = 1.017 q_{F3} = -0.339	C-C C-F	0.262 0.292	-0.622 -0.511	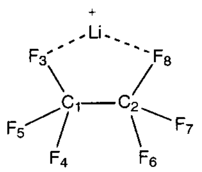	q_{C1} = 1.021 q_{F3} = -0.430 q_{F4} = -0.282 q_{F5} = -0.299 q_{Li^+} = 0.979	C1-C2 C1-F3 C1-F4 C1-F5 F3-Li^+	0.257 0.242 0.319 0.310 0.225	-0.592 -0.464 -0.499 -0.513 0.163
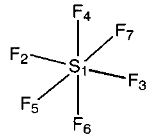	q_{S1} = 2.633 q_{F2} = -0.439	S-F	0.217	-0.208	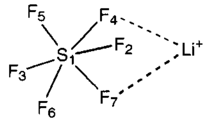	q_{S1} = 2.631 q_{F2} = -0.406 q_{F4} = -0.509 q_{F5} = -0.391 q_{Li^+} = 0.981	S1-F2 S1-F4 S1-F5 F4-Li^+	0.227 0.181 0.237 0.218	-0.188 -0.177 -0.117 0.157
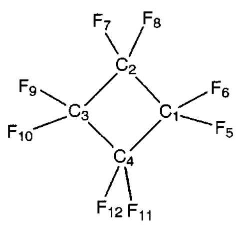	q_{C1} = 0.668 q_{F5} = -0.334	C-C C1-F5 C1-F6	0.245 0.279 0.283	-0.515 -0.317 -0.299	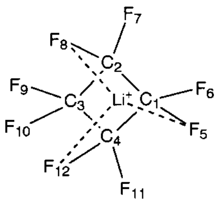	q_{C1} = 0.664 q_{C2} = 0.674 q_{C3} = 0.683 q_{F5} = -0.392 q_{F6} = -0.284 q_{F7} = -0.282 q_{F8} = -0.403 q_{F9} = -0.307 q_{Li^+} = 0.969	C1-C2 C2-C3 C1-F5 C1-F6 C2-F7 C2-F8 C3-F9 F5-Li^+ F8-Li^+	0.244 0.242 0.252 0.304 0.308 0.243 0.292 0.193 0.171	-0.509 -0.501 -0.302 -0.284 -0.255 -0.308 -0.350 0.135 0.118

electron density, and electron-density Laplacian of monomers have been tabulated in Table 2. *ρ* at the bond critical point increases from CH_3F to CF_4 and reveals the strengthening of the bond. It is also evident from the $\nabla^2\rho$ values that the covalency of the C−F bond increases (increase in $\nabla^2\rho$ value, in the negative scale).

From the stability trend of these four ligands, one can expect that the less stable molecule in this series interacts more strongly with the Li^+ ion and the opposite may be true for the most stable molecule. Table 1 shows that the Li^+ ion affinity increases with the decrease in fluorine number. The Li^+ ion affinity of tetrafluoromethane is 12.31 kcal/mol, while that for fluoromethane is 30.10 kcal/mol, both obtained at the B3LYP/6-311+G(3df) level of theory. So the affinity values are as follows $CF_4 < CHF_3 < CH_2F_2 < CH_3F$. As we mentioned earlier, the Li^+ ion affinities calculated for CH_2F_2 and CH_3F agree well

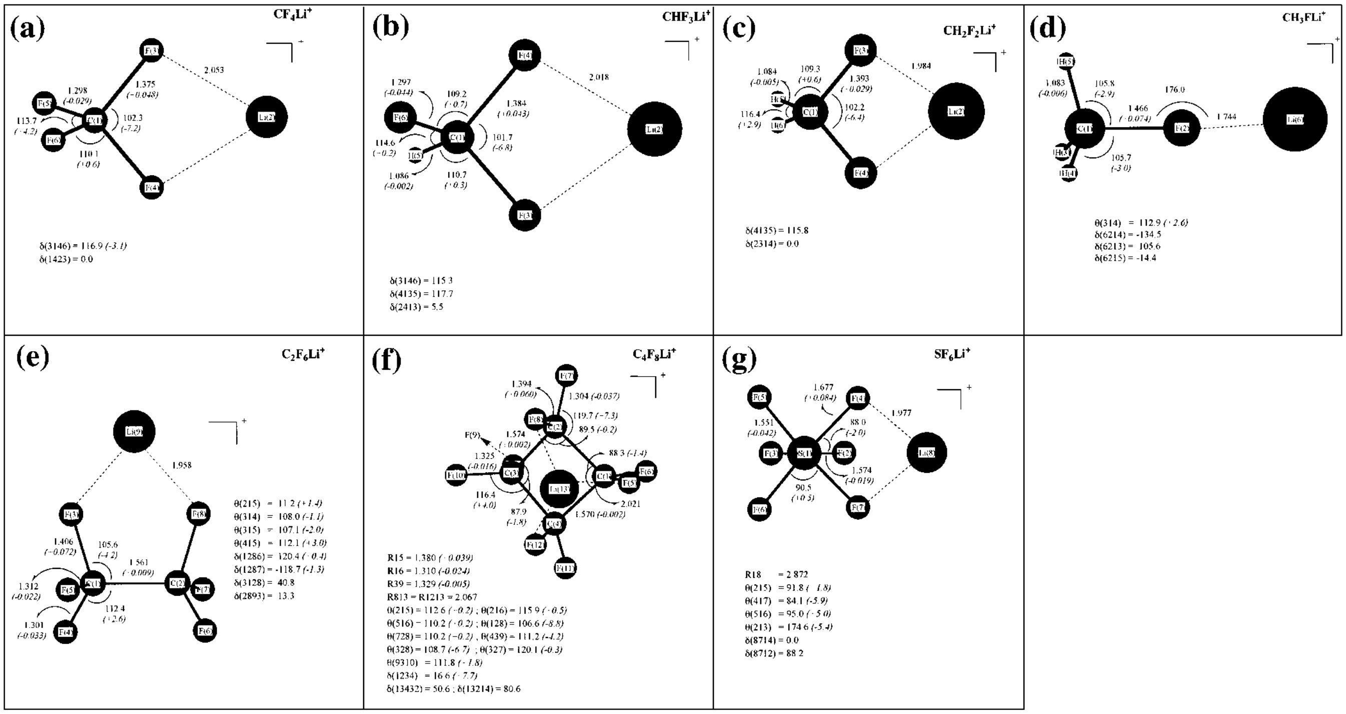

Figure 1. Complex structure, values in the parentheses represent changes in ligand geometries upon complexation. All the values are obtained at B3LYP/6-311+G(2d).

with the experimental values. The corresponding affinity values for CHF_3 and CF_4 molecules are 19.64 and 12.31 kcal/mol, respectively. CF_4 does not have a dipole or quadrupole moment,[54] and its electric dipole polarizability is small.[55] Hence, there is a weaker interaction between CF_4 and the Li^+ ion. The Li^+ ion affinity obtained for tetrafluoromethane is twice the binding energy of the CF_4-F^- complex (6.4 kcal/mol, C_{3v} symmetry),[56] which reveals that CF_4 is comparatively favorable for positive ion interactions, in spite of the presence of a cationic central carbon atom. The bond distance (R) between the Li^+ ion and the interacting fluorine atoms is directly correlated with the affinity of the molecules. The R value decreases with the increase in affinities.

Some interesting results were obtained in the complex structures (Figure 1a−d). The optimized [at B3LYP/6-311+G(2d)] complex structures with the changes in structural parameters of the ligands upon Li^+ ion attachment are given in Figure 1a−d. Some of structures were particularly interesting, especially the CF_4-Li^+ and CHF_3-Li^+ complexes. The monomer symmetry of these two molecules changed upon their respective Li^+ attachment. The tetrahedral CH_4 became a C_{3v} structure when it formed the CH_4-Li^+ complex;[57] however, the CF_4 molecule, which has the same tetrahedral structure, became C_{2v} symmetry while forming the CF_4-Li^+ complex (Figure 1a). The CHF_3-Li^+ complex has C_s symmetry (Figure 1b) rather than a C_{3v} symmetry. This may be due to the fact that in the CH_4-Li^+ case, the Li^+ ion interacts with the central carbon atom, while in the CF_4-Li^+ complex it cannot interact in the same way because the carbon atom is highly cationic. Therefore, the Li^+ ion shares its interaction with two fluorine atoms. The shape of the fluorine atomic orbitals also played a vital role in the symmetry change. Almost all the selected PFCs interacted in the same way with Li^+ ions, i.e., two fluorine atoms shared interaction with the Li^+ ion. So there is no change in symmetry due to CH_2F_2 complexation with the Li^+ ion, i.e., C_{2v} symmetry, for both ligand and the complex (Figure 1c). It is worth noting that the CH_3F-Li^+ complex does not have a C_{3v} symmetry structure (Figure 1d); the bond angle for $C-F-Li^+$ is 176°.

The ρ and $\nabla^2\rho$ study was used to analyze the bonding nature between the Li^+ ion and the ligand in a complex. It may also be used to understand the change in chemical bonding in ligands (bond activation) upon association with the Li^+ ion. The calculated atomic charges, electron densities, and Laplacian electron densities (the latter two obtained at bond critical points) for ligands, as well as complexes, are depicted in Table 2. Upon ion association, the ligands become polarized toward the ion and due to its higher electronegativity nature, the interacting fluorine atom draws some charge away from their counterparts. So in the presence of less electronegative hydrogen atoms, the charge drawing power of the fluorine atom increases in association with an increase in hydrogen numbers and thus in the CH_3F-Li^+ complex, it becomes more negatively charged than the respective fluorine atoms in other complexes. This polarization and the change in electronic charge of each atomic center is reflected in the change in ligand bond lengths upon complexation. The C−F (interacting with the ion) bond length increases by 0.048 Å, while the nonbonding C−F bond length decreases by 0.029 Å in CF_4. This increase in C−F bond length is greater (0.074 Å) in the CH_3F-Li^+ complex.

However, direct conclusions cannot be drawn by comparing the electronic charge on Li^+ in the complexes with their interaction energies. The Li^+ ion in the CH_3F-Li^+ complex retains its atomic charge of 0.990 e, while in the CF_4-Li^+ complex, it is 0.982 e. Charge transfer in the latter is larger than that in the former, but the Li^+ affinity of the CH_3F is larger. However, ρ and $\nabla^2\rho$ show good correlation with the ion affinity of the molecules. Examination of the ρ values at bcp(C−F) reveals that the density depopulated in the ion interacting C−F bonds and further populated in the ion-non-interacting C−F bonds in complexes when compared with the respective C−F bonds in the ligands. The change in $\nabla^2\rho$ values at bcp of the interacting C−F bonds upon complexation is directly proportional to the bond weakening. This shows the superiority of these parameters in analyzing the bond. The study reveals that the ρ and $\nabla^2\rho$ values at the Li^+-F bond critical points have a good correlation with the Li^+ ion affinities of the ligands. Li^+ ion affinity increases with increases in electron density and Laplacian electron density at Li^+-F bcp. The increase in ρ at Li^+-F bcp makes a stronger lone pair−ion interaction and thus, higher affinity. The ρ and $\nabla^2\rho$ values at the Li^+-F critical points in CF_4-Li^+ are 0.176 e/au^3 and 0.123 e/au^5, respectively, while in the CH_3F-Li^+ complex they are 0.373 e/au^3 and 0.341 e/au,^{5} respectively. Therefore, in similar molecules, bcp parameters, ρ and $\nabla^2\rho$, can be used to quantify bond activation in ligands upon ion association and importantly, may provide information about ion affinities of base molecules. The electronic properties of the $F-Li^+$ bcps suggest a weak bonding interaction with low ρ and small positive $\nabla^2\rho$ values, all indicative of closed-shell-type electrostatic interactions. Worth noting is that there was a moderate charge concentration along the ion−molecular interaction bond path in the CH_3F-Li^+ complex, when compared to the other three complexes.

(b) C_2F_6 and C_4F_8. Since both molecules have no permanent electric dipole moment[58] in association with very small polarizability, one cannot expect very large Li^+ ion affinities for these compounds. The affinity values calculated for C_2F_6 and C_4F_8 at B3LYP/6-311+G(3df) level were 17.20 and 21.09 kcal/mol, respectively (Table 1).

The geometry of these complexes show some interesting features (Figure 1e,f). In both cases, the carbon atoms are cationic in nature because of the presence of more electronegative fluorine atoms thus generating different complex structures. Li^+ ion interacts with two fluorine atoms through the C_{2v} symmetry axis, as shown in Figure 1e, since the highest filled orbital in the ground state of C_2F_6 is mainly populated in the C−C bond.[59] It is interesting to note that the staggered D_{3d} symmetry C_2F_6 forms C_{2v} symmetry $C_2F_6-Li^+$. The δ(F3C1C2F8) decreases by around 20° (see Figure 1e). The dihedral angle between $CFLi^+$ and FLi^+F planes is 13.3°. As expected, due to Li^+ ion association, the C−C bond length slightly increases (0.009 Å); however, the largest bond elongation (0.072 Å) occurs in the C−F bond, which interacts with the ion and the bond contraction in the other two ion-non-interacting C−F bonds. All the other changes are summarized in Figure 1e.

Because of its well-known carbon ring puckering nature, octafluorocyclobutane belongs to the D_{2d} symmetry point group in its ground state[60] (Figure 1f). The Li^+ ion interacts with three fluorine atoms of the C_4F_8 ligand. Upon Li^+ ion attachment, the puckering angle of the carbon ring increased by 7.7°. According to this complex structure, there were some changes in the ligand structure (see Figure 1f).

The calculated ρ and $\nabla^2\rho$ values at bond critical points for both ligands, as well as complexes, are given in Table 2. The ρ at C−C bcp slightly decreased with the complex formation and shows electron density was not depopulated at C−C bcp in a larger extent, accordingly there should be a very small decrease in covalency. However, ρ values at bcp(C−F), the C−F bonds interacting with the Li^+ ion, decreased upon ion association, reflecting its depletion in the bond path, while in the noninteracting C−F bonds, the electron density increased at the bcp(C−F) and bond strengthening was observed. Table 2 shows these changes clearly. Laplacian also accounts for these changes. These ρ and $\nabla^2\rho$ values at the bcp($F-Li^+$) reflect the bonding nature of these complexes. Again, these small ρ and $\nabla^2\rho$ values are ideal for closed shell electrostatic interactions.

(c) SF_6. Quantitative analysis of bonding in the hypervalent SF_6 compound by Reed and Weinhold[61] reveals that the essential features of binding are well-described by an ionic donor−acceptor $S^{3+}(F^{0.5-})_6$ picture. As we have seen in the PFCs, due to the large electronegativity difference between the central S and F atoms, SF_6 has a large ionic character and the central S atom is highly cationic. Like many of the PFCs, SF_6 does not have permanent electric dipole moment, while its polarizability is large. But because of high symmetry, O_h, and the well-known electron scavenger nature, SF_6 may have smaller ion affinity. The calculated Li^+ ion affinity was 16.92 kcal/mol at B3LYP/6-311+G(3df) level.

As expected, the Li^+ ion interacts with two of the SF_6 fluorine atoms. The complex geometry associated with the change in structural parameters of the ligand due to the Li^+ ion association are given in Figure 1g. The equivalence of six S−F bonds is broken by the ion attachment. The θ(F4S1F7) lessened by 5.9°. Figure 1g shows the ion interacting S−F bonds changes significantly (+0.084 Å) when compared with the other S−F bonds (−0.042 and −0.019 Å) upon complexation.

The ρ and $\nabla^2\rho$ values at S−F bond critical points for ligands as well as complexes are given in Table 2. The changes in the ρ and $\nabla^2\rho$ values clearly describe the changes in the bonding behaviors. Again the ρ and $\nabla^2\rho$ values calculated at $F-Li^+$ bcp show that the ion−molecular interaction is a dipole-induced electrostatic interaction.

Conclusions

The larger Li^+ ion affinities obtained for the perfluorocarbons evaluated here reveal that lithiated PFCs can be detected in our Li^+-ion attachment mass spectrometry. This work supports our ongoing experimental setup for the quantification of PFC gas emission from semiconductor industries.

Li^+ ion affinities of CF_4, CHF_3, C_2F_6, C_4F_8, and SF_6 molecules were obtained for the first time. The Li^+ ion affinities calculated for CH_3F and CH_2F_2 molecules compare well with the experimental results. Some of the complex structures differ from similar complexes formed between hydrocarbons and Li^+ ions. Examination of atomic charges and bond analysis using Bader's Atoms-in-Molecules theory demonstrated that the ion−molecular association is mainly due to dipole-induced electrostatic interactions.

Acknowledgment. One of the authors (S.A) expresses his sincere thanks to the Japan Science and Technology Agency for the award of a Postdoctoral Fellowship.

References and Notes

(1) EPA National Air Pollutant Emissions Trends Report, 1900−1996. The 1998 Report of the U.S. Environmental Protection Agency.

(2) Intergovernmental Panel on Climate Change (IPCC). The 1994 Report of the Scientific Assessment Working Group of IPCC.

(3) See the references in refs 12−14.

(4) Ravishankara, A. R.; Soloman, S.; Turnipseed, A. A.; Warren, R. F. *Science* **1993**, *259*, 194.

(5) Ramanathan, V.; Callis, L.; Cess, R.; Hansen, J.; Isaksen, I.; Kuhn, W.; Lacis, A.; Luther, F.; Mahlman, J.; Reck, R.; Schlesinger, M. *Rev. Geophys.* **1987**, *25*, 1441.

(6) Stolarski, R. S.; Rundel, R. D. *Geophys. Res. Lett.* **1975**, *2*, 443.

(7) Noutary, C. J. *J. Res. Natl. Bur. Stand. Sec. A* **1968**, *72*, 479.

(8) Winters, H. F. In *Swarm Studies and Inelastic Electron−Molecule Collisions*; Pitchford, L. C., McKoy, B. V., Chutjian, A., Trajmar, S., Eds.; Springer: New York, 1987; p 347.

(9) Winters, H. F.; Inokuti, M. *Phys. Rev. A* **1982**, *25*, 1420.

(10) Stephan, K.; Deutsch, H.; Mark, T. D. *J. Chem. Phys.* **1985**, *83*, 5712.

(11) Brehm, B.; Frey, R.; Kustler, A.; Eland, J. H. D. *Int. J. Mass. Spectrom. Ion Phys.* **1974**, *13*, 251.

(12) Christophorou, L. G.; Olthoff, J. K.; Rao, M. V. V. S. *J. Phys. Chem. Ref. Data* **1996**, *25*, 1341.

(13) Christophorou, L. G.; Olthoff, J. K.; Rao, M. V. V. S. *J. Phys. Chem. Ref. Data* **1997**, *26*, 1.

(14) Christophorou, L. G.; Olthoff, J. K. *J. Phys. Chem. Ref. Data* **1998**, *27*, 1.

(15) Harnisch, J.; Borchers, R.; Fabian, P.; Maiss, M. *Geophys. Res. Lett.* **1996**, *23*, 1099.

(16) Fujii, T.; Ogura, M.; Jimba, H. *Anal. Chem.* **1989**, *61*, 1026.

(17) Fujii, T.; Syouji, K. *Phys. Rev. A* **1991**, *46*, 3555.

(18) Fujii, T. *Anal. Chem.* **1992**, *64*, 775.

(19) Fujii, T. *Chem. Phys. Lett.* **1992**, *191*, 162.

(20) Fujii, T.; Syouji, K. *J. Appl. Phys.* **1993**, *74*, 3009.

(21) Fujii, T.; Syouji, K. *J. Phys. Chem.* **1993**, *97*, 11380.

(22) Fujii, T.; Syouji, K. *Phys. Rev. E* **1994**, *49*, 657.

(23) Fujii, T.; Ohta, M. *J. Phys. D. Appl. Phys.* **1995**, *28*, 1268.

(24) Fujii, J. *J. Appl. Phys.* **1997**, *82*, 2056.

(25) Fujii, T.; Kim, H. S. *Chem. Phys. Lett.* **1997**, *268*, 229.

(26) Fujii, T.; Yashiro, Y.; Tokiwa, H.; Soma, Y. *J. Am. Chem. Soc.* **1997**, *119*, 12280.

(27) Fujii, T. *Phys. Rev. E* **1998**, *58*, 6495.

(28) Fujii, T. *Chem. Phys. Lett.* **1999**, *313*, 733.

(29) Fujii, T.; Arai, N. *Astrophys. J.* **1999**, *519*, 858.

(30) Dzidic, I.; Kebarle, P. *J. Phys. Chem.* **1970**, *74*, 1466.

(31) Staley, R. H.; Beauchamp, J. L. *J. Am. Chem. Soc.* **1975**, *97*, 5920.

(32) Kollman, P.; Rotherberg, S. *J. Am. Chem. Soc.* **1977**, *99*, 1333.

(33) Del Bene, J. E.; Frisch, M. J.; Raghavachari, K.; Pople, J. A.; Schleyer, P. v. R. *J. Phys. Chem.* **1983**, *87*, 73.

(34) Parr, R. G.; Yang, W. *Annu. Rev. Chem*. **1995**, *46*, 701, and references therein.

(35) Stockigt, D. *Chem. Phys. Lett.* **1996**, *250*, 387.

(36) Remko, M. *Mol. Phys.* **1997**, *91*, 929.

(37) Miklis, P. C.; Ditchfield, R.; Spencer, T. A. *J. Am. Chem. Soc*. **1998**, *120*, 10482.

(38) Bader, R. F. W.; Essen, H. *J. Chem. Phys.* **1984**, *80*, 1943.

(39) Bader, R. F. W.; MacDougall, P. J.; Lau, C. D. H. *J. Am. Chem. Soc.* **1984**, *106*, 1594.

(40) Wiberg, K. B.; Bader, R. F. W.; Lau, C. D. H. *J. Am. Chem. Soc.* **1987**, *109*, 985.

(41) Bader, R. F. W. *Atoms in Molecules. A Quantum Theory*; Oxford University Press: New York, 1990.

(42) Frisch, M. J.; Trucks, G. W.; Schlegel, H. B.; Scuseria, G. E.; Robb, M. A.; Cheeseman, J. R.; Zakrzewski, V. G.; Montgomery, J. A.; Stratmann, R. E.; Burant, J. C.; Dapprich, S.; Millam, J. M.; Daniels, A. D.; Kudin, K. N.; Strain, M. C.; Farkas, O.; Tomasi, J.; Barone, V.; Cossi, M.; Cammi, R.; Mennucci, B.; Pomelli, C.; Adamo, C.; Clifford, S.; Ochterski, J.; Petersson, G. A.; Ayala, P. Y.; Cui, Q.; Morokuma, K.; Malick, D. K.; Rabuck, A. D.; Raghavachari, K.; Foresman, J. B.; Cioslowski, J.; Ortiz, J. V.; Stefanov, B. B.; Liu, G.; Liashenko, A.; Piskorz, P.; Komaromi, I.; Gomperts, R.; Martin, R. L.; Fox, D. J.; Keith, T.; Al-Laham, M. A.; Peng, C. Y.; Nanayakkara, A.; Gonzalez, C.; Challacombe, M.; Gill, P. M. W.; Johnson, B. G.; Chen, W.; Wong, M. W.; Andres, J. L.; Head-Gordon, M.; Replogle, E. S.; Pople, J. A. *Gaussian 98, Revision A.7*; Gaussian, Inc.: Pittsburgh, PA, 1998.

(43) Becke, A. D. *J. Chem. Phys.* **1993**, *98*, 5648.

(44) Lee, C.; Yang, W.; Parr, R. G. *Phys. Rev. B* **1988**, *37*, 785.

(45) Pople, J. A.; Head-Gordon, M.; Fox, D. J.; Raghavachari, K.; Curtiss, L. A. *J. Chem. Phys.* **1989**, *98*, 5622. Curtiss, L. A.; Jones, C.; Tuckers, G. W.; Raghavachari, K.; Pople, J. A. *J. Chem. Phys.* **1990**, *93*, 2537.

(46) Reed, A. E.; Weinstock, R. B.; Weinhold, F. *J. Chem. Phys.* **1985**, *83*, 735.

(47) Reed, A. E.; Curtiss. L. A.; Weinhold, F. *Chem. Rev.* **1986**, *86*, 899.

(48) Salzner, U.; Schleyer, P.v. R. *Chem. Phys. Lett.* **1992**, *190*, 401.

(49) Wiberg, K. B.; Rablen, P. R. *J. Am. Chem. Soc.* **1993**, *115*, 614, and references therein.

(50) Dill, J. D.; Schleyer, P.v. R.; Pople, J. A. *J. Am. Chem. Soc.* **1976**, *98*, 1663.

(51) Schleyer, P.v. R.; Kos, A. J. *Tetrahedron* **1983**, *39*, 1141.

(52) Hehre, W. J.; Ditchfield, R.; Radom, L.; Pople, J. A. *J. Am. Chem. Soc.* **1970**, *92*, 4796.

(53) Reed, A. E.; Schleyer, P.v. R. *J. Am. Chem. Soc.* **1987**, *109*, 7362.

(54) Brundle, C. R.; Robin, M. B.; Basch, H. *J. Chem. Phys.* **1970**, *53*, 2196.

(55) Beran, J. A.; Kevan, L. *J. Phys. Chem.* **1969**, *73*, 3860.

(56) Hiraoka, K.; Nasu, M.; Fujimaki, S.; Ignacio, E. W.; Yamabe, S. *Chem. Phys. Lett.* **1995**, *245*, 14.

(57) Arulmozhiraja, S.; Fujii, T.; Tokiwa, H. *Chem. Phys.* **1999**, *250*, 237.

(58) McClellan, A. L. *Tables of Experimental Dipole Moments*; W. H. Freeman and Company: San Francisco, CA, 1963; p 51.

(59) Sauvageau, P.; Doucet, J.; Gilbert, R.; Sandorfy, C. *J. Chem. Phys.* **1974**, *61*, 391.

(60) Fischer, G.; Purchase, R. L.; Smith, D. M. *J. Mol. Struct.* **1997**, *405*, 159.

(61) Reed, A. E.; Weinhold, F. *J. Am. Chem. Soc.* **1986**, *108*, 3586.